Alkyladenine DNA glycosylase (AAG) localizes to mitochondria and interacts with mitochondrial single-stranded binding protein (mtSSB)

Citation: Van Loon, Barbara, and Leona D. Samson. "Alkyladenine DNA Glycosylase (AAG) Localizes to Mitochondria and Interacts with Mitochondrial Single-Stranded Binding Protein (mtSSB)." DNA Repair 12, no. 3 (March 2013): 177–187.

As Published: http://dx.doi.org/10.1016/j.dnarep.2012.11.009

Publisher: Elsevier

Persistent URL: http://hdl.handle.net/1721.1/99514

Version: Author's final manuscript: final author's manuscript post peer review, without publisher's formatting or copy editing

Published in final edited form as:
DNA Repair (Amst). 2013 March 1; 12(3): 177–187. doi:10.1016/j.dnarep.2012.11.009.

Alkyladenine DNA glycosylase (AAG) localizes to mitochondria and interacts with mitochondrial single-stranded binding protein (mtSSB)

Barbara van Loon[1,2,5] and **Leona D. Samson**[1,2,3,4]

[1]Department of Biological Engineering, Massachusetts Institute of Technology, Cambridge, Massachusetts 02139, USA [2]Department of Biology, Massachusetts Institute of Technology, Cambridge, Massachusetts 02139, USA [3]Center for Environmental Health Sciences, Massachusetts Institute of Technology, Cambridge, Massachusetts 02139, USA [4]David H. Koch Institute for Integrative Cancer Research, Massachusetts Institute of Technology, Cambridge, Massachusetts 02139, USA [5]Institute of Veterinary Biochemistry and Molecular Biology, University of Zürich, Winterthurerstrasse 190, CH-8057 Zürich, Switzerland

Abstract

Due to a harsh environment mitochondrial genomes accumulate high levels of DNA damage, in particular oxidation, hydrolytic deamination, and alkylation adducts. While repair of alkylated bases in nuclear DNA has been explored in detail, much less is known about the repair of DNA alkylation damage in mitochondria. Alkyladenine DNA glycosylase (AAG) recognizes and removes numerous alkylated bases, but to date AAG has only been detected in the nucleus, even though mammalian mitochondria are known to repair DNA lesions that are specific substrates of AAG. Here we use immunofluorescence to show that AAG localizes to mitochondria, and we find that native AAG is present in purified human mitochondrial extracts, as well as that exposure to alkylating agent promotes AAG accumulation in the mitochondria. We identify mitochondrial single-stranded binding protein (mtSSB) as a novel interacting partner of AAG; interaction between mtSSB and AAG is direct and increases upon methyl methanesulfonate (MMS) treatment. The consequence of this interaction is specific inhibition of AAG glycosylase activity in the context of a single-stranded DNA (ssDNA), but not a double-stranded DNA (dsDNA) substrate. By inhibiting AAG-initiated processing of damaged bases, mtSSB potentially prevents formation of DNA breaks in ssDNA, ensuring that base removal primarily occurs in dsDNA. In summary, our findings suggest the existence of AAG-initiated BER in mitochondria and further support a role for mtSSB in DNA repair.

Corresponding Author: Leona D. Samson, Massachusetts Institute of Technology, 56-235, 77 Massachusetts Avenue, Cambridge, MA 02139, USA, Tel.: (617) 258-7813, Fax: (858) 784-2779, lsamson@mit.edu.

Conflict of Interest: The authors declare that there is no conflict of interest.

Keywords

mitochondria; base excision repair; alkyladenine DNA glycosylase; mitochondrial single-stranded binding protein

1. Introduction

The human mitochondrial genome comprises 16,569 DNA base pairs, organized in a circular, double-stranded DNA (dsDNA) molecule. *In vivo* two to eight mitochondrial DNA (mtDNA) molecules are held together in a protein-DNA complex known as the mitochondrial nucleoid [1]. Proteins involved in nucleoid formation include mitochondrial single-stranded binding protein (mtSSB), DNA polymerase (pol)!, mtDNA helicase (Twinkle) and mitochondrial transcription factor A (TFAM) [2, 3]. Similar to the nuclear genome, mtDNA is continuously exposed to various DNA damaging agents. Due to high levels of reactive oxygen species (ROS) generated within mitochondria, frequently occurring DNA lesions include products of oxidation and hydrolytic deamination, as well as exocyclic adducts, like 1,N^6-ethenoadenine (!A), formed indirectly through lipid peroxidation [4-6]. In comparison to the nuclear genome, mtDNA accumulates more damage after treatment with alkylating or oxidative agents [7-11]. The importance of mtDNA maintenance is clearly demonstrated by numerous findings associating mutations in the mitochondrial genome with a plethora of human pathologies [12, 13]. In addition to giving rise to inherited diseases [12, 14], mutations in mtDNA have been strongly linked to cancer, aging and diabetes [15-17].

To prevent accumulation of small DNA base lesions, cells utilize the base excision repair (BER) pathway. DNA glycosylases determine the specificity of this pathway by recognizing and excising specific damaged bases, generating an abasic (AP) site that is processed by the apurinic/apyrimidinic endonuclease 1 (APE1); the resulting gap is filled and sealed by DNA pol and DNA ligase, respectively [18-20]. To date six DNA glycosylases are known to localize in mitochondria; 8-oxoguanine DNA glycosylase (OGG1), MutY homologue (MutYH), uracil DNA glycosylase 1 (UNG1), Nth endonuclease III-like 1 (NTH1) and two endonuclease VIII homologs (NEIL1 and NEIL2) [21-29]. These DNA glycosylases process a variety of DNA base lesions, including 7,8-dihydro-8-oxo-2′deoxyguanine (8-oxo-G), uracil (U) and 5-hydroxyuracil (5OHU).

The DNA glycosylase that usually recognizes and excises alkylated and deaminated bases from DNA is the alkyladenine DNA glycosylase (AAG) [30]. Gene encoding human AAG is positioned on the short arm of the chromosome 16 and comprises five exons, of which two (1a and 1b) are localized in the promoter region [31]. Since the promoter activity has been detected only upstream of exon 1a and not in the DNA region between the two exons, it is suggested that three distinct mRNA forms of human AAG, are formed through post-transcriptional processing [32]. Isoform A is the longest transcript; isoform B lacks an exon in the 5′ region and is translated from an alternative start codon [31, 33, 34]. Isoform C is the shortest transcript variant that is missing part of the 5′coding region and is translated from a downstream in-frame start codon [35]. AAG has a unique ability among DNA glycosylases to act on several structurally diverse bases within dsDNA, such as: 3-

methyladenine, 7-methyguanine, hypoxanthine (Hx), !A, 1-methylguanine, 1,N^2-ethenoguanine and U [35-39]. Besides lesions in dsDNA, AAG can also remove !A and Hx from single-stranded DNA (ssDNA), thereby creating AP sites that could potentially give rise to harmful DNA breaks [37]. To our knowledge, AAG has not previously been detected in the mitochondria, despite the fact that mammalian mitochondria have been shown to repair DNA lesions that are specific substrates of AAG [40-42].

In addition to the major BER enzymes, several auxiliary proteins have been implicated in mitochondrial BER, such as mtSSB and TFAM. Both mtSSB and TFAM inhibit removal of the damaged bases from mtDNA [43, 44]. The presence of mtSSB impairs UNG1 mediated excision of U and 5OHU from ssDNA [44]. MtSSB also inhibits ssDNA nicking by APE1 [44]. Besides potential involvement in DNA repair, the primary role of mtSSB is in mtDNA replication, during which it stimulates the activity of DNA pol ! and helicase Twinkle, as well as influencing displacement-loop (D-loop) turnover [45-49]. The D-loop is a triple stranded structure generated during strand displacement mtDNA replication [50, 51]. The consequence of such strand-asymmetric DNA synthesis is that one of the newly synthetized mitochondrial genomes contains large ssDNA regions [52-55]. Binding of the mtSSB homotetramer to ssDNA is of crucial importance to ensure genomic stability and to prevent formation of highly toxic and mutagenic DNA lesions, such as DNA breaks [56, 57]. Although mtSSB inhibits removal of U and 5OHU from ssDNA, thus preventing subsequent formation of DNA breaks, it is not clear whether this effect is UNG1 specific, or if mtSSB plays a more general role in inhibiting mitochondrial BER initiation by influencing other DNA glycosylases.

Here we analyzed the localization of human AAG in different cellular compartments. In addition to the nucleus and cytoplasm, we detected AAG in the mitochondria. Exposure to methyl methanesulfonate (MMS) promoted mitochondrial accumulation of AAG. Software analysis identified potential mitochondrial targeting signal (MTS) in two of the three known AAG isoforms, further supporting our finding that AAG localizes in the mitochondria. To explore which mitochondrial proteins associate with AAG, we performed liquid chromatography-mass spectrometry (LC-MS) and identified mtSSB in complex with AAG. We confirmed direct physical interaction between AAG and mtSSB, and observed that the extent of interaction is dependent on MMS treatment. Finally we demonstrate that mtSSB significantly dampens AAG activity in the context of ssDNA, but does not affect AAG mediated processing of damaged substrate in dsDNA. MtSSB thus potentially regulates AAG activity in mitochondria by: (i) preventing AAG-mediated removal of alkylation damage from ssDNA, thus averting the formation of extremely harmful DNA breaks; and (ii) ensuring that AAG-mediated processing of DNA base lesions takes place only upon reestablishment of dsDNA. In summary, our findings suggest the existence of AAG in the mitochondria and further support an important role of mtSSB in mtDNA repair.

2. Material and Methods

2.1. Chemicals

Labeled ! [^{32}P] ATP was purchased from Perkin Elmer and Hartmann Analytic. All the other reagents were of analytical grade and purchased from Merck, Sigma or Fluka. The

undamaged 39-mer and complementary 16-mer oligonucleotides were purchased from Microsynth.

2.2. Oligonucleotide DNA Substrates

16-mer oligonucleotide containing !A lesion or undamaged A was kindly provided by Prof. John M. Essigman. Synthesis of these oligonucleotides was performed as described previously [58]. The sequence of the 16-mer oligonucleotide containing !A lesion or undamaged A is depicted in the Fig. 4A. The control 39-mer oligonucleotide sequence was published before [59]. Primers were 5′-labeled with ![^{32}P] ATP using T4 polynucleotide kinase (New England Biolabs), according to the manufacturer's protocol. For experiments involving dsDNA substrates, complementary 16-mer oligonucleotides were annealed using a 1:1.5 ratio of modified to unlabeled complement. As a base opposite !A lesion was chosen thymine (T), the base-paring partner of the undamaged base.

2.3. Cells and cell treatments

Human HEK293T and HeLa CCL2 cells were purchased from American Tissue Type Culture Collection and grown in a humidified 5% CO2 atmosphere in DMEM containing GlutaMAX-I supplemented with 10% FBS and 100U/ml penicillin-streptomycin (all obtained from Gibco, Invitrogen).

Treatment of cells with alkylating agent was achieved by incubation for 1h at 37°C in serum-free DMEM containing 2mM MMS or serum-free medium alone (mock treatment).

Double thymidine block was accomplished by seeding HeLa CCL2 cells in six-well plates containing complete DMEM medium for 8h, after which medium with 2mM thymidine was added and cells incubated for 16h. Cells were next washed with phosphate-buffered saline (PBS) and incubated for 8h in fresh medium, followed by second 16h incubation in medium with 2mM thymidine. Synchronization of cells at G1/S boundary was confirmed by fluorescence activated cell sorting analysis as described before [59].

2.4. Whole cell extracts

Cells were trypsinized, washed twice with cold PBS and resuspended in two packed cell volumes (PCV) of hypotonic lysis buffer (20mM HEPES at pH7.9, 2mM $MgCl_2$, 0.2mM EGTA, 10% (v/v) glycerol, 0.1mM PMSF, 2mM DTT) complemented with Halt Protease and Phosphatase Inhibitors Single-Use Cocktail without EDTA (Thermo Scientific). After swelling for 5min at 4°C, cells were lysed by three freeze/thaw cycles. NaCl and Nonidet-P40 were added next to a final concentration 0.5M and 0.5% (v/v), respectively and incubated 20min at 4°C. Samples were diluted with eight PCV of lysis buffer containing 50mM NaCl, sonicated and centrifuged. The supernatants were flash frozen in liquid N_2 or analyzed directly.

2.5. Isolation of mitochondria from HEK293T cells

Human mitochondria were isolated from HEK293T cells according to a well-established protocol [60]. Briefly, 2mM MMS or mock treated cells were harvested and washed twice with cold PBS. Cell pellet was resuspended in six PCV of homogenization medium (10mM

Tris-HCl at pH 6.7, 0.15mM $MgCl_2$, 10mM KCl) and homogenized using a tightly fitting Dounce homogenizer. The homogenate was complemented with two PCV of homogenization medium containing 1M sucrose and nuclei were pelleted by centrifugation 5min at 1000g, 4°C. The pellet was washed in homogenization medium, centrifuged and nuclear extract prepared by the addition of TXIP buffer (10mM Tris-HCL at pH 7.8, 150mM NaCl, 1% Triton X-100, 1mM EDTA, 1mM DTT, 0.25mM PMSF, 10% (v/v) glycerol). The supernatant obtained upon pelleting of nuclei was transferred to a fresh tube and centrifuged a second time for 10min at 5000g, 4°C. The supernatant was collected, representing the cytoplasmic fraction, while the pellet was resuspended in sucrose/Mg^{2+} medium (10mM Tris-HCl at pH 6.7, 0.15mM $MgCl_2$, 0.25M sucrose) and centrifuged for 10min at 5000g, 4°C. The pelleted mitochondria were resuspended in TXIP buffer. All protein concentrations were determined by BioRad assay using BSA as standard.

2.6. Mitochondrial trypsin digestion

After centrifugation in sucrose/Mg^{2+} medium, purified mitochondria were treated with 1, 5 and 10 μg/ml trypsin (Sigma) in 100μl of digestion medium (10mM Tris-HCl at pH 7.4, 0.1mM EGTA, and 0.25M sucrose) for 1h at 4 °C. The reaction was stopped by addition of 50μg Leupeptin and the mitochondria were centrifuged at 18000g for 5 min. Mitochondrial extracts were obtained by resuspending pellet in TXIP buffer, loaded on an SDS-PAGE gel and subjected to immunoblot analysis.

2.7. Protein analysis

Purified protein samples, nuclear, mitochondrial, cytoplasmic and whole cellular extracts were separated on 4–12% Bis–Tris polyacrylamide gels (Invitrogen) followed by transfer to Immobilon-FL membrane (Millipore) for immunoblotting or silver staining (SilverQuest Kit, Invitrogen). Primary antibodies against the FLAG tag (F1804, Sigma), mtSSB (ab74710, Abcam), AAG (rabbit polyclonal antibody generated in our laboratory; or sc-101237, Santa Cruz), PCNA (sc-56, Santa Cruz), GAPDH (sc-69778, Santa Cruz), Lamin B (101-B7, Calbiochem), VDAC1 (sc-32063, Santa Cruz), Mitofilin (ab110329, Abcam) and mtHSP70 (ab2799, Abcam) were detected using infrared (IR) Dye-conjugated secondary antibodies (Rockland). The signal was visualized using direct IR fluorescence via the Odyssey Scanner (LI-COR Biosciences).

2.8. Microscopy

HeLa CCL2 cells were grown on glass coverslips and synchronized by double thymidine block. Upon release cells were incubated for 30min at 37°C in DMEM medium containing 100nM CMXRos-MitoTracker (Invitrogen). Cells were then washed with PBS and mock or MMS treated for 1h at 37°C. After the treatment cells were allowed to recover for 1h at 37°C in full medium. Treated cells were fixed with 3.7% paraformaldehyde for 10min and permeabilized with 0.1% Triton in 1× CSK buffer (100mM NaCl, 300mM sucrose, 10mM PIPES, 3mM $MgCl_2$, 1mM EGTA) for 15min at room temperature. To block non-specific binding samples were incubated with 4%BSA in PBS with 0.1% Nonidet-P40 for 1h at 37°C. Primary AAG antibody (HPA006531, Sigma) diluted 1:60 in PBS was added to samples and incubated over-night at 4°C. After extensive washing, samples were incubated with fluorophore-conjugated secondary antibody (ab6717, Abcam) at room temperature for

2h. After washing off the unbound antibody ProLong Gold Antifade reagent (Invitrogen) was used according to the manufacturers protocol. Images were captured with the Nikon eclipse E800 with attached Qimaging retina exi fast 1394 camera.

2.9. Expression and purification of human ! 80AAG, ! 16mtSSB, Cdk1 and PCNA

Human recombinant !80AAG protein was expressed and purified as described previously [61]. The first 80 amino acids were deleted from the N-terminus to facilitate protein purification. ! 80AAG is a well-characterized variant of AAG, with a catalytic activity very similar to that of the full-length protein [35, 61]. To express human mtSSB protein, *Escherichia coli* BL21(DE3) strain (Novagen) was transfected with pET21aHmtSSB construct, encoding human mtSSB protein, lacking 16 N-terminal amino acids. The expression construct was a kind gift from Dr. William C. Copeland (NIEHS, USA). Expression and purification were performed according to previously established protocol [62]. Deletion of 16 amino acids, encoding mitochondrial targeting signal, from the N-terminus of mtSSB was shown not to affect mtSSB properties, such as tetramerisation and binding of ssDNA [62]. The protein concentrations depicted in different figures of this manuscript are calculated for mtSSB as a tetrameric protein. Human PCNA and Cdk1 have been expressed and purified as described previously [63, 64].

2.10. Expression and purification of human full-length AAG

The coding region of full-length human AAG (NCBI: NP_002425.2) was amplified and cloned into a modified pcDNA3.1 vector (Invitrogen) containing a triple Flag-streptavidin binding peptide fusion protein [65], resulting in N-terminally Flag-Tag fused AAG expression construct. Empty pcDNA3.1-Flag or pcDNA3.1-FlagAAG expression constructs (0.1! g/ml) were transiently transfected into 293T human embryonic kidney cells by calcium phosphate precipitation. Before harvesting, cells were mock treated or treated with 2mM MMS for 1h and whole cell extracts were prepared. Whole cell extracts (1mg total protein) were incubated with 20! l of FLAG M2 antibody resin (Sigma) for 2h at 4°C in wash buffer (20mM HEPES at pH7.9, 2mM $MgCl_2$, 0.2mM EGTA, 10% (v/v) glycerol, 0.1mM PMSF, 2mM DTT, 140mM NaCl, 0.01% (v/v) Nonidet-P40). The resin was washed four times using the same buffer. Bound samples were eluted in two steps with wash buffer containing 100! g/mL 3×Flag peptide (Sigma) and flash frozen in liquid N_2 or subjected to trichloroacetic acid precipitation.

2.11. Protein mass spectrometry

Protein identification was performed by the Biopolymers and Proteomics Core Facility of the David H. Koch Institute for Integrative Cancer Research (http://ki.mit.edu/sbc/biopolymers). Briefly, protein samples were reduced, alkylated, and digested with trypsin, followed by purification and desalting on an analytical C_{18} column tip. Processed peptides were analyzed by chromatography on an Agilent Model 1100 Nanoflow high-pressure liquid chromatography (HPLC) system coupled with electrospray ionization on a Thermo Electron Model LTQ Ion Trap mass spectrometer. Scaffold (version Scaffold_3_00_04, Proteome Software Inc., Portland, OR) was used to validate MS/MS based peptide and protein identifications. Peptide identifications were accepted if they could be established at greater

than 95.0% probability as specified by the Peptide Prophet algorithm [66]. Peptide identifications were also required to exceed specific database search engine thresholds. SEQUEST [67] identification required spectra to match full tryptic peptides of at least 7 amino acids, have a normalized difference in cross-correlation scores (ΔCn) of at least 0.1, and have minimum cross-correlation scores (Xcorr) of greater than 2.0, 2.5, 3.5 and 3.5 for singly, doubly, triply and quadruply charged peptides. Protein identifications were accepted if they could be established at greater than 99.0% probability and contained at least 2 identified peptides.

2.12. Immunoprecipitation

Whole cell extracts (0.5mg of total protein) were incubated with 2! g of AAG antibody (sc-101237, Santa Cruz) or normal mouse IgG (sc-2343) at 4°C over night. Protein A Dynabeads (Invitrogen) were equilibrated in the wash buffer (20mM HEPES at pH7.9, 2mM $MgCl_2$, 0.2mM EGTA, 10% (v/v) glycerol, 0.1mM PMSF, 2mM DTT, 140mM NaCl, 0.01% (v/v) Nonidet-P40) and blocked at 4°C over night in a wash buffer containing 1% BSA. After three consecutive washes using wash buffer, beads were added to samples containing WCE and antibody; and incubated for 4,5h at 4°C. The supernatant was removed and beads washed three times with cold wash buffer. Beads were boiled in Laemmli sample loading buffer, resolved on 4-12% SDS-PAGE gel and subjected to immunoblot analysis.

2.13. Far Western Blotting

Detection of protein-protein interactions by far western blotting was performed according to a previously established protocol [68]. Briefly, purified recombinant ! 80AAG, His tagged ! 16mtSSB, BSA, GST tagged Cdk1 and His tagged PCNA (1! g) were separated by SDS-PAGE and transferred onto a polyvinylidene fluoride (PVDF) membrane. Membranes were then briefly stained by Ponceau to ensure equal loading, followed by destaining. Proteins were denatured and renatured *in situ* in AC buffer (10% (v/v) glycerol, 100mM NaCl, 20mM Tris at pH 7.5, 1mM EDTA, 0.1% (v/v) Tween-20, 2% (w/v) milk, 1mM DTT) by gradually reducing the guanidine-HCl concentration from 6M to 0M. Renatured membranes were blocked with 5% milk in PBST, followed by incubation with purified interacting (bait) protein ! 80AAG or ! 16mtSSB, as indicated in Fig. 3 legends, at a concentration of 1! g/ml in PB buffer (20mM HEPES at pH7.9, 2mM $MgCl_2$, 10% (v/v) glycerol, 0.1mM PMSF, 1mM DTT, 130mM NaCl, 0.01% (v/v) Nonidet-P40), overnight at 4°C. To ensure specificity of obtained results in the negative control samples 1! g/ml of BSA was added to PB buffer and incubated with membrane overnight at 4°C. Unbound protein was removed in four washing steps using PB buffer. In the second wash PB buffer was complemented with 0.0001% (v/v) glutaraldehyde. From this point a conventional immunoblot analysis was performed with the respective antibodies.

2.14. DNA Glycosylase Assay

For denaturing gel analysis of DNA glycosylase products, the reaction mixture (10! l) containing: 20mM Tris-HCl at pH7.8, 100mM KCl, 5mM 2-mercaptoethanol, 2mM EDTA, 1mM EGTA, 50! g/ml BSA and 2nM ^{32}P-labelled DNA substrate was incubated with 200nM ! 80AAG. Amounts of recombinant BSA and human ! 16mtSSB were varied as

indicated in the figure legends. In all DNA glycosylase assays an extensively characterized form of AAG lacking the first 80 amino acids was used. The experiments were performed under single-turnover conditions, with an enzyme concentration 100-fold higher than the amount of labeled DNA oligonucleotide. Reaction mixtures were incubated 30min at 37°C. For kinetics studies, an aliquot of the reaction mixture was removed for quenching 0, 5, 15, 30, 45, 60, 90, 120 and 180min after the initiation of the reaction. Reactions were quenched with 0.2N NaOH and heated for 15 min at 75°C. Formamide loading buffer was added to each sample and cleaved products resolved on a 20% denaturing polyacrylamide gel. Products of the DNA glycosylase assay were visualized by PhosphorImager (Typhoon Trio, GE Healthcare) and analyzed by ImageQuant and GelEval 1.35 scientific imaging software (FrogDance Software, UK). Enzymatic rate constants were determined using GraphPad Prisam (GraphPad Software, Inc., La Jolla, CA) by fitting the gel band intensities of single-turnover kinetics experiments into OnePhase Exponential Association equitation:

$$y = y_{\max}(1 - e^{-k\ t}_{obs}) \quad (1)$$

where y is the amount of substrate cleaved at any particular time point, y_{max} represents the maximum amount of cleaved substrate, t is time and k_{obs} is the observed activity rate constant.

2.15. Electrophoretic Mobility Shift Assay

The binding affinity of ! 80AAG and ! 16mtSSB was tested in a reactions containing 50mM HEPES at pH7.5, 100mM NaCl, 1mM EDTA, 5mM DTT, 25! g/ml BSA, 9.5% (v/v) glycerol and and 2nM ^{32}P-labelled DNA. The amounts of recombinant human ! 80AAG and ! 16mtSSB were as indicated in the figure legends. Reactions were incubated for 30min at 4°C and directly loaded on a 6% nondenaturing polyacrylamide gel. The separated products were visualized as described above for DNA glycosylase activity assay.

3. Results

3.1. Human AAG Localizes to the Mitochondria, Nucleus, and Cytoplasm, and its Cellular Distribution is Affected by MMS Treatment

To determine localization of human AAG in different cellular compartments, we fractioned human HEK293T cells. Immunoblot analysis of nuclear, cytoplasmic and mitochondrial fractions, reveals that AAG is not only present in the nucleus and cytoplasm, but also localizes to the mitochondria (Fig. 1A, lane 3). To confirm that AAG is present in the mitochondria, and to ensure that the observed effect is not a result of mitochondrial purification procedure, we performed a trypsin digestion assay (Fig. 1B). Treatment of isolated mitochondria with increasing trypsin induces gradual degradation of the proteins closest to mitochondrial surface, followed by degradation of proteins in the matrix. Though increasing trypsin amount partially affects AAG levels, Fig. 1B clearly shows that under conditions that induce complete disruption of outer and inter mitochondrial membrane proteins, namely VDAC1 and Mitofilin respectively, portion of AAG persists in the mitochondrial matrix fraction marked by the presence of mtHSP70 (Fig. 1B, lane 4). Complete loss of AAG and mtHSP70 signal is observed only upon treatment of isolated

mitochondria with SDS (Fig. 1B, lane 5). These findings indicate that the protease-resistant AAG fraction resides in the mitochondria, while the fraction digested by trypsin is present in the external mitochondrial compartments, and confirm the conclusion from Fig. 1A that AAG is a mitochondrial protein. We next tested whether exposure to alkylating agent MMS influences AAG protein levels in the mitochondria isolated from cells immediately upon the treatment and at different times post treatment. Exposure to MMS induces a moderate increase in mitochondrial AAG protein levels, directly after the treatment (Fig. 1C, lane 2 and Fig. 1D), suggesting that induction of DNA alkylation damage promotes rapid accumulation of AAG. Similar to the effect observed in mitochondria, MMS treatment leads to a slight increase in nuclear AAG levels, albeit with different kinetics; AAG reaches a maximum 0.5h after the exposure (Fig. S1A and B). In contrast to the mitochondria and nucleus, levels of AAG in the cytoplasm remain largely unchanged upon MMS exposure (Fig. S1C and D). These findings are further supported by immunofluorescence analysis, which indicates that, although the majority of AAG localizes in the nucleus, a portion of AAG clearly localizes in the mitochondria (Fig. 1E). The amount of AAG signal in mitochondria is further increased upon MMS treatment (Fig. 1F). As this is the first time that localization of endogenous AAG has been observed in mitochondria, we next addressed which of the three AAG isoforms has the potential to be targeted to this cellular compartment. Three software programs; MitoProt II [69], PSORT II [70] and iPSORT [71] predict that isoforms A and B most likely localize to the mitochondria (Table 1). MitoProt II and iPSORT software further indicate that isoforms A and B could be synthesized as a precursor containing a MTS of 17 and 12 amino acids, respectively (Table 1). Taken together these data indicate that AAG has the potential to localize into mitochondria.

3.2. MtSSB is detected in complex with human AAG

To better understand the potential role of AAG in mitochondria we tested whether any of the proteins known to localize in this cellular compartment associate with AAG. We expressed, and tandem affinity purified, the Flag-tagged human AAG isoform A protein from untreated or MMS treated HEK293T cells. This isoform was chosen since *in silico* analysis predicted that it contains a MTS. In parallel, a mock purification was performed from cells transfected with empty vector. Silver staining and immunoblot analysis indicate that tagged AAG was present in the appropriate cells (Fig. 2A and B). The empty vector and AAG samples from untreated and MMS treated cells were next subjected to LC-MS. PCNA, a known interacting partner of AAG [72] was found specifically in both AAG containing samples (Fig. 2C). Only one protein that localizes specifically in the mitochondria co-purified with AAG, namely mtSSB (Fig. 2C). In contrast to PCNA, mtSSB peptides are detected only in the MMS-pretreated cells (Fig. 2C). We infer either that AAG and mtSSB interact specifically upon treatment with alkylating agent, or that in untreated cells the amount of mtSSB associated with AAG is not detectable by LC-MS.

3.3. Human AAG and mtSSB Proteins Directly Interact

To address whether mtSSB and AAG can interact in the absence of DNA damaging agent, and whether mtSSB and AAG interact under conditions when AAG is not ectopically expressed, we performed AAG-immunoprecipitation assays using untreated, non-transfected human cells. Incubation of the AAG antibody with whole cell extract resulted in the

immunoprecipitation of mtSSB in complex with AAG (Fig. 3A, lane 2), thus indicating that AAG and mtSSB form a complex at endogenous levels under normal conditions. We next determined whether MMS exposure affects the intensity of interaction between these two proteins. The highest level of mtSSB co-immunoprecipitating with AAG is observed directly after the MMS treatment (Fig. 3A, lane 3), and this level diminishes with time (Fig. 3A, lanes 4-6). These results correlate well with the observed increase in the mitochondrial AAG protein levels directly after MMS exposure (Fig. 1C and D). In addition, the stronger interaction observed between AAG and mtSSB upon exposure to alkylation damage, may explain why, by LC-MS, we only detected mtSSB in the fractions collected immediately after MMS treatment and not in the untreated sample (Fig. 2C). To exclude the possibility that the difference in the interaction intensity may be a consequence of changes in protein levels, we analyzed whole cell extracts by immunoblot analysis; we did not detect any significant changes in either mtSSB or AAG levels upon MMS treatment (Fig. S2). Since endogenous AAG and mtSSB could potentially form a complex indirectly through a mutual association with DNA, we next used far western blotting to determine whether mtSSB and AAG interact directly. For these experiments we used two well-characterized truncated recombinant protein forms ! 16mtSSB and ! 80AAG, neither of which contain a predicted MTS, ensuring that the MTS could not mediate protein-protein interaction and that the AAG/mtSSB complex could exist in the mitochondria. ! 80AAG, BSA as a negative control, and the known mtSSB interacting partner Cdk1 [73], were immobilized on a PVDF membrane (Fig 3B), followed by *in situ* renaturation. The membrane was then incubated with a solution of 1! g/ml ! 16mtSSB, washed and any bound protein detected using mtSSB antibody (Fig 3C). The presence of a mtSSB signal at the positions of ! 80AAG and Cdk1 indicates that ! 16mtSSB directly interacts with these two proteins (Fig 3C). Using a reverse approach with ! 16mtSSB immobilized to PVDF membrane (Fig 3D), followed by incubation with 1! g/ml ! 80AAG solution and protein detection with AAG antibody gave similar result; AAG was detected at the position of ! 16mtSSB, as well as at the position of PCNA, but not at the position of BSA (Fig 3E). These far western experiments with purified proteins clearly show that AAG directly binds to mtSSB (Fig. 3C and E).

3.4. MtSSB Inhibits AAG Activity

Having shown that mtSSB and AAG directly interact, we went on to explore whether this interaction affects AAG activity. We performed all experiments under single-turnover conditions to ensure that a single AAG molecule binds and acts only once on damaged DNA. We chose a ssDNA 16-mer oligonucleotide as a substrate (Fig. 4A). A short DNA oligonucleotide was used to minimize binding of mtSSB to the substrate; human mtSSB is known to cooperatively bind 50-70 nucleotides of DNA per tetramer [74]. The 16-mer AAG oligonucleotide substrate contained an !A lesion (Fig. 4A), known to be induced in mitochondria and to be linked to mitochondrial instability and apoptosis [4]. Upon titration of ! 16mtSSB in the DNA glycosylase assay we observe that ! 16mtSSB inhibits ! 80AAG mediated removal of ! A from ssDNA, when the amount of mtSSB is equal to the amount of DNA glycosylase present in the reaction (Fig. 4B, compare lane 6 with 2). This effect is statistically significant (Fig. 4C) and specific, since under the same conditions, titration of BSA does not affect ! 80AAG glycosylase activity (Fig. S3). Finding that ! 16mtSSB significantly inhibits ! 80AAG activity only when equal amounts of proteins are used,

indicates that inhibition is potentially a result of direct protein-protein interaction. However, it is formally possible that ! 16mtSSB binds to the short ssDNA under our assay conditions, preventing DNA glycosylase from accessing the damaged base. To distinguish between the two, and to confirm that mtSSB does not bind efficiently to the 16-mer ssDNA, we performed electrophoretic mobility shift analysis. In agreement with previous findings [75], ! 16mtSSB is fully functional and binds efficiently to 39-mer ssDNA, but is not able to stably associate with undamaged 16-mer oligonucleotide (Fig. S4A), Further titration of ! 16mtSSB alone or in the presence of ! 80AAG does not result in a distinct binding of the ! 16mtSSB to the !A containing 16-mer ssDNA (Fig. S4B). Taken together our results thus suggest that mtSSB inhibits AAG mediated processing of damaged DNA through direct protein-protein interaction.

3.5. Inhibition of AAG Activity by mtSSB Occurs Specifically in the Context of Single-Stranded, but not Double-Stranded DNA

AAG is known to recognize and excise !A lesions from both ssDNA and dsDNA [58]. To address if mtSSB, inhibits AAG activity on dsDNA as it does in the context of ssDNA, we performed kinetic experiments. AAG activity was measured under single-turnover conditions in the absence or presence of ! 16mtSSB, equimolar to the amount of DNA or ! 80AAG. Kinetic experiments clearly indicate that while ! 16mtSSB, under equimolar protein conditions, efficiently inhibits ! 80AAG glycosylase activity on ssDNA, (Fig. 5A, lanes 13-18; and Fig. 5C), it has absolutely no effect the excision of damaged base from dsDNA substrate (Fig. 5B, lanes 13-18; and Fig. 5D). In the presence of equimolar mtSSB, the AAG-mediated initial excision rate constant on ssDNA is reduced 1.92-fold, but the activity rate is unaffected (Table 2). Taken together these findings confirm that the inhibitory effect observed on ssDNA is a result of protein-protein interaction and further suggest that mtSSB specifically prevents formation of AP sites within ssDNA that could potentially lead to formation of harmful DNA breaks. By inhibiting AAG-initiated processing of damaged bases within ssDNA, mtSSB ensures that lesion removal only occurs upon reestablishment of dsDNA.

4. Discussion

As a byproduct of energy production in mitochondria, extremely high levels of DNA damaging species are generated; some of the frequently occurring mtDNA lesions are products of oxidation and hydrolytic deamination, as well as !-base adducts [4-6]. An increase in the rate of hydrolytic deamination of adenine to Hx correlates with an increased likelihood of A → G transition mutations in mtDNA [76]. In addition, high levels of !A in mtDNA coincide with increased mitochondrial instability and apoptosis [4]. AAG is known to efficiently recognize and remove both Hx and !A from nuclear DNA. Although mammalian mitochondrial extracts are able to excise Hx and !-base adducts from DNA, so far AAG has not been detected in mitochondria [40-42, 77]. Here we report the presence of AAG in human mitochondrial extracts and propose that mtSSB protein influences AAG-initiated BER. Upon exposure of cells to MMS we observe a moderate accumulation of AAG in the mitochondria directly after treatment, while increases in the level of nuclear AAG occur at later time points (Fig. 1C and S1A). These findings suggest that AAG

mediated base excision in the mitochondrial genome may occur faster than that in nuclear DNA. This is in agreement with previous observations that mtDNA lesions are repaired more rapidly than damages present in the nucleus [78]. In addition, cellular exposure to oxidizing or alkylating agents gives rise to a higher density of mtDNA lesions compared to nuclear DNA [7-11], indicating a need to repair mitochondrial damage promptly and efficiently. *In silico* analysis of three AAG isoforms predicts the presence of a MTS in two of them, namely isoforms A and B (Table 1). Accordingly, these two isoforms also have a high probability to be targeted into mitochondria (Table 1). To confirm localization of both isoforms A and B in this cellular compartment, understand how is their import regulated, as well as if localization of these two proteins is timely separated or if they act simultaneously remains to be addressed in future studies. In order to better understand the function of AAG isoform A in the mitochondria, we tested whether any mitochondrial protein interacts with AAG. MtSSB specifically and directly associates with AAG (Fig. 3). The intensity of the interaction is modulated upon MMS exposure and correlates with the amount of AAG observed in the mitochondria. As a consequence of direct interaction, ! 16mtSSB inhibits ! 80AAG-mediated processing of damaged ssDNA, but has no effect on lesion removal from the dsDNA (Fig. 5). How the interaction of AAG with mtSSB leads to specific inhibition of AAG activity within ssDNA and not dsDNA, may potentially be answered at the level of lesion recognition. In dsDNA, recognition of the damaged nucleotide is a highly organized process mediated through nucleotide flipping out of the DNA duplex into the active site of AAG [36]. Due to lack of base pairing and reduced base stacking in ssDNA it has been suggested that in ssDNA the damaged base is more loosely captured in the AAG active site [37]. AAG may thereby remove an ! A lesion from ssDNA without tightly binding to it [37]. In the dsDNA however, AAG mediated processing of an ! A lesion occurs through strong association with the duplex substrate [37]. It is thus possible that by interacting with AAG, mtSSB prevents lesion recognition, while in dsDNA recognition and removal of the damaged base is not affected due to tight binding of AAG to damaged dsDNA. Very recently, mtSSB was reported to associate with another BER glycosylase, UNG1 [44]. Similar to its effect on AAG, mtSSB interacts directly with UNG1 and specifically inhibits removal of U from ssDNA, but not from dsDNA [44]. Together, these observations suggest an important role for mtSSB in mitochondrial BER. Besides its involvement in mtDNA replication, where mtSSB binds and protects large ssDNA regions, mtSSB potentially also preserves the integrity of smaller ssDNA gaps. Though mtSSB does not efficiently bind to very short ssDNA, by physically associating and inhibiting DNA glycosylases, mtSSB could prevent the formation of AP sites and subsequent formation of extremely harmful DNA breaks in the DNA gaps. Binding of mtSSB to (i) large ssDNA regions generated during DNA replication, as well as (ii) inhibition of lesion processing within small gaps, through interaction with DNA glycosylases, are potentially crucial mechanisms for preventing the formation of DNA breaks, as well counteracting the loss of genetic information [52-55]. MtSSB may thus serve as a BER regulator, ensuring that processing of damaged bases occurs only upon the reestablishment of dsDNA. Our results suggest the existence of novel AAG-initiated BER in mitochondria that is regulated by mtSSB. The significance of this pathway in human cells is demonstrated through finding that targeted overexpression of AAG in mitochondria strongly sensitizes breast cancer cells to chemotherapeutic agents

[79]. Future studies are needed to understand the details of AAG-initiated BER in mitochondria, with a potential to reveal new targets to combat cancer.

Supplementary Material

Refer to Web version on PubMed Central for supplementary material.

Acknowledgments

We thank Dr. Jenifer A. Calvo and Dr. Dragony Fu for stimulating discussions and helpful suggestions. We are very grateful to; Prof. John M. Essigmann for the DNA oligonucleotide containing ! A lesion, Dr. Dragony Fu for creating pcDNA3.1.-FlagAAG expression vector, Dr. Manjappa Lingaraju Gondichatnahalli for purifying ! 80AAG enzyme and Dr. William C. Copeland for kindly providing pET21aHmtSSB expression construct. This work was funded by NIH grants CA055042 and ES002109 and is supported by University of Zurich. L.D.S. is an American Cancer Society Research Professor.

References

1. Legros F, Malka F, Frachon P, Lombes A, Rojo M. Organization and dynamics of human mitochondrial DNA. J Cell Sci. 2004; 117:2653–2662. [PubMed: 15138283]
2. Wang Y, Bogenhagen DF. Human mitochondrial DNA nucleoids are linked to protein folding machinery and metabolic enzymes at the mitochondrial inner membrane. J Biol Chem. 2006; 281:25791–25802. [PubMed: 16825194]
3. Rebelo AP, Williams SL, Moraes CT. In vivo methylation of mtDNA reveals the dynamics of protein-mtDNA interactions. Nucleic Acids Res. 2009; 37:6701–6715. [PubMed: 19740762]
4. Nair J, Strand S, Frank N, Knauft J, Wesch H, Galle PR, Bartsch H. Apoptosis and age-dependant induction of nuclear and mitochondrial etheno-DNA adducts in Long-Evans Cinnamon (LEC) rats: enhanced DNA damage by dietary curcumin upon copper accumulation. Carcinogenesis. 2005; 26:1307–1315. [PubMed: 15790590]
5. Ichikawa J, Tsuchimoto D, Oka S, Ohno M, Furuichi M, Sakumi K, Nakabeppu Y. Oxidation of mitochondrial deoxynucleotide pools by exposure to sodium nitroprusside induces cell death. DNA Repair (Amst). 2008; 7:418–430. [PubMed: 18155646]
6. Ohno M, Oka S, Nakabeppu Y. Quantitative analysis of oxidized guanine, 8-oxoguanine, in mitochondrial DNA by immunofluorescence method. Methods Mol Biol. 2009; 554:199–212. [PubMed: 19513676]
7. Zastawny TH, Dabrowska M, Jaskolski T, Klimarczyk M, Kulinski L, Koszela A, Szczesniewicz M, Sliwinska M, Witkowski P, Olinski R. Comparison of oxidative base damage in mitochondrial and nuclear DNA. Free Radic Biol Med. 1998; 24:722–725. [PubMed: 9586801]
8. Yakes FM, Van Houten B. Mitochondrial DNA damage is more extensive and persists longer than nuclear DNA damage in human cells following oxidative stress. Proc Natl Acad Sci U S A. 1997; 94:514–519. [PubMed: 9012815]
9. LeDoux SP, Wilson GL, Beecham EJ, Stevnsner T, Wassermann K, Bohr VA. Repair of mitochondrial DNA after various types of DNA damage in Chinese hamster ovary cells. Carcinogenesis. 1992; 13:1967–1973. [PubMed: 1423864]
10. Myers KA, Saffhill R, O'Connor PJ. Repair of alkylated purines in the hepatic DNA of mitochondria and nuclei in the rat. Carcinogenesis. 1988; 9:285–292. [PubMed: 3338112]
11. Wunderlich V, Schutt M, Bottger M, Graffi A. Preferential alkylation of mitochondrial deoxyribonucleic acid by N-methyl-N-nitrosourea. Biochem J. 1970; 118:99–109. [PubMed: 5472159]
12. Tuppen HA, Blakely EL, Turnbull DM, Taylor RW. Mitochondrial DNA mutations and human disease. Biochim Biophys Acta. 2010; 1797:113–128. [PubMed: 19761752]
13. Copeland WC. Defects in mitochondrial DNA replication and human disease. Crit Rev Biochem Mol Biol. 2012; 47:64–74. [PubMed: 22176657]

14. Chan SS, Copeland WC. DNA polymerase gamma and mitochondrial disease: understanding the consequence of POLG mutations. Biochim Biophys Acta. 2009; 1787:312–319. [PubMed: 19010300]
15. Lee HC, Wei YH. Mitochondria and aging. Adv Exp Med Biol. 2012; 942:311–327. [PubMed: 22399429]
16. Boesch P, Weber-Lotfi F, Ibrahim N, Tarasenko V, Cosset A, Paulus F, Lightowlers RN, Dietrich A. DNA repair in organelles: Pathways, organization, regulation, relevance in disease and aging. Biochim Biophys Acta. 2011; 1813:186–200. [PubMed: 20950654]
17. Chatterjee A, Mambo E, Sidransky D. Mitochondrial DNA mutations in human cancer. Oncogene. 2006; 25:4663–4674. [PubMed: 16892080]
18. Dalhus B, Laerdahl JK, Backe PH, Bjoras M. DNA base repair--recognition and initiation of catalysis. FEMS Microbiol Rev. 2009; 33:1044–1078. [PubMed: 19659577]
19. Jacobs AL, Schar P. DNA glycosylases: in DNA repair and beyond. Chromosoma. 2011
20. Liu P, Demple B. DNA repair in mammalian mitochondria: Much more than we thought? Environ Mol Mutagen. 2010; 51:417–426. [PubMed: 20544882]
21. Nilsen H, Otterlei M, Haug T, Solum K, Nagelhus TA, Skorpen F, Krokan HE. Nuclear and mitochondrial uracil-DNA glycosylases are generated by alternative splicing and transcription from different positions in the UNG gene. Nucleic Acids Res. 1997; 25:750–755. [PubMed: 9016624]
22. Nishioka K, Ohtsubo T, Oda H, Fujiwara T, Kang D, Sugimachi K, Nakabeppu Y. Expression and differential intracellular localization of two major forms of human 8-oxoguanine DNA glycosylase encoded by alternatively spliced OGG1 mRNAs. Mol Biol Cell. 1999; 10:1637–1652. [PubMed: 10233168]
23. Takao M, Zhang QM, Yonei S, Yasui A. Differential subcellular localization of human MutY homolog (hMYH) and the functional activity of adenine:8-oxoguanine DNA glycosylase. Nucleic Acids Res. 1999; 27:3638–3644. [PubMed: 10471731]
24. Ohtsubo T, Nishioka K, Imaiso Y, Iwai S, Shimokawa H, Oda H, Fujiwara T, Nakabeppu Y. Identification of human MutY homolog (hMYH) as a repair enzyme for 2-hydroxyadenine in DNA and detection of multiple forms of hMYH located in nuclei and mitochondria. Nucleic Acids Res. 2000; 28:1355–1364. [PubMed: 10684930]
25. Ikeda S, Kohmoto T, Tabata R, Seki Y. Differential intracellular localization of the human and mouse endonuclease III homologs and analysis of the sorting signals. DNA Repair (Amst). 2002; 1:847–854. [PubMed: 12531031]
26. Karahalil B, de Souza-Pinto NC, Parsons JL, Elder RH, Bohr VA. Compromised incision of oxidized pyrimidines in liver mitochondria of mice deficient in NTH1 and OGG1 glycosylases. J Biol Chem. 2003; 278:33701–33707. [PubMed: 12819227]
27. Hashiguchi K, Stuart JA, de Souza-Pinto NC, Bohr VA. The C-terminal alphaO helix of human Ogg1 is essential for 8-oxoguanine DNA glycosylase activity: the mitochondrial beta-Ogg1 lacks this domain and does not have glycosylase activity. Nucleic Acids Res. 2004; 32:5596–5608. [PubMed: 15494448]
28. Hu J, de Souza-Pinto NC, Haraguchi K, Hogue BA, Jaruga P, Greenberg MM, Dizdaroglu M, Bohr VA. Repair of formamidopyrimidines in DNA involves different glycosylases: role of the OGG1, NTH1, and NEIL1 enzymes. J Biol Chem. 2005; 280:40544–40551. [PubMed: 16221681]
29. Mandal SM, Hegde ML, Chatterjee A, Hegde PM, Szczesny B, Banerjee D, Boldogh I, Gao R, Falkenberg M, Gustafsson CM, Sarkar PS, Hazra TK. Role of human DNA glycosylase Nei-like 2 (NEIL2) and single strand break repair protein polynucleotide kinase 3′-phosphatase in maintenance of mitochondrial genome. J Biol Chem. 2012; 287:2819–2829. [PubMed: 22130663]
30. Fu D, Calvo JA, Samson LD. Balancing repair and tolerance of DNA damage caused by alkylating agents. Nat Rev Cancer. 2012; 12:104–120. [PubMed: 22237395]
31. Vickers MA, Vyas P, Harris PC, Simmons DL, Higgs DR. Structure of the human 3-methyladenine DNA glycosylase gene and localization close to the 16p telomere. Proc Natl Acad Sci U S A. 1993; 90:3437–3441. [PubMed: 8475094]

32. Izumi T, Tatsuka M, Tano K, Asano M, Mitra S. Molecular cloning and characterization of the promoter of the human N-methylpurine-DNA glycosylase (MPG) gene. Carcinogenesis. 1997; 18:1837–1839. [PubMed: 9328183]
33. Samson L, Derfler B, Boosalis M, Call K. Cloning and characterization of a 3-methyladenine DNA glycosylase cDNA from human cells whose gene maps to chromosome 16. Proc Natl Acad Sci U S A. 1991; 88:9127–9131. [PubMed: 1924375]
34. Chakravarti D, Ibeanu GC, Tano K, Mitra S. Cloning and expression in Escherichia coli of a human cDNA encoding the DNA repair protein N-methylpurine-DNA glycosylase. J Biol Chem. 1991; 266:15710–15715. [PubMed: 1874728]
35. O'Connor TR. Purification and characterization of human 3-methyladenine-DNA glycosylase. Nucleic Acids Res. 1993; 21:5561–5569. [PubMed: 8284199]
36. Lau AY, Wyatt MD, Glassner BJ, Samson LD, Ellenberger T. Molecular basis for discriminating between normal and damaged bases by the human alkyladenine glycosylase, AAG. Proc Natl Acad Sci U S A. 2000; 97:13573–13578. [PubMed: 11106395]
37. Lee CY, Delaney JC, Kartalou M, Lingaraju GM, Maor-Shoshani A, Essigmann JM, Samson LD. Recognition and processing of a new repertoire of DNA substrates by human 3-methyladenine DNA glycosylase (AAG). Biochemistry. 2009; 48:1850–1861. [PubMed: 19219989]
38. Miao F, Bouziane M, O'Connor TR. Interaction of the recombinant human methylpurine-DNA glycosylase (MPG protein) with oligodeoxyribonucleotides containing either hypoxanthine or abasic sites. Nucleic Acids Res. 1998; 26:4034–4041. [PubMed: 9705516]
39. Saparbaev M, Laval J. Excision of hypoxanthine from DNA containing dIMP residues by the Escherichia coli, yeast, rat, and human alkylpurine DNA glycosylases. Proc Natl Acad Sci U S A. 1994; 91:5873–5877. [PubMed: 8016081]
40. Pirsel M, Bohr VA. Methyl methanesulfonate adduct formation and repair in the DHFR gene and in mitochondrial DNA in hamster cells. Carcinogenesis. 1993; 14:2105–2108. [PubMed: 8222061]
41. Pettepher CC, LeDoux SP, Bohr VA, Wilson GL. Repair of alkali-labile sites within the mitochondrial DNA of RINr 38 cells after exposure to the nitrosourea streptozotocin. J Biol Chem. 1991; 266:3113–3117. [PubMed: 1825207]
42. LeDoux SP, Driggers WJ, Hollensworth BS, Wilson GL. Repair of alkylation and oxidative damage in mitochondrial DNA. Mutat Res. 1999; 434:149–159. [PubMed: 10486589]
43. Canugovi C, Maynard S, Bayne AC, Sykora P, Tian J, de Souza-Pinto NC, Croteau DL, Bohr VA. The mitochondrial transcription factor A functions in mitochondrial base excision repair. DNA Repair (Amst). 2010; 9:1080–1089. [PubMed: 20739229]
44. Wollen Steen K, Doseth B, M PW, Akbari M, Kang D, Falkenberg M, Slupphaug G. mtSSB may sequester UNG1 at mitochondrial ssDNA and delay uracil processing until the dsDNA conformation is restored. DNA Repair (Amst). 2012; 11:82–91. [PubMed: 22153281]
45. Korhonen JA, Gaspari M, Falkenberg M. TWINKLE Has 5′ -> 3′ DNA helicase activity and is specifically stimulated by mitochondrial single-stranded DNA-binding protein. J Biol Chem. 2003; 278:48627–48632. [PubMed: 12975372]
46. Farr CL, Wang Y, Kaguni LS. Functional interactions of mitochondrial DNA polymerase and single-stranded DNA-binding protein. Template-primer DNA binding and initiation and elongation of DNA strand synthesis. J Biol Chem. 1999; 274:14779–14785. [PubMed: 10329675]
47. Genuario R, Wong TW. Stimulation of DNA polymerase gamma by a mitochondrial single-strand DNA binding protein. Cell Mol Biol Res. 1993; 39:625–634. [PubMed: 8054997]
48. Oliveira MT, Kaguni LS. Reduced stimulation of recombinant DNA polymerase gamma and mitochondrial DNA (mtDNA) helicase by variants of mitochondrial single-stranded DNA-binding protein (mtSSB) correlates with defects in mtDNA replication in animal cells. J Biol Chem. 2011; 286:40649–40658. [PubMed: 21953457]
49. Takamatsu C, Umeda S, Ohsato T, Ohno T, Abe Y, Fukuoh A, Shinagawa H, Hamasaki N, Kang D. Regulation of mitochondrial D-loops by transcription factor A and single-stranded DNA-binding protein. EMBO Rep. 2002; 3:451–456. [PubMed: 11964388]
50. Arnberg A, van Bruggen EF, Borst P. The presence of DNA molecules with a displacement loop in standard mitochondrial DNA preparations. Biochim Biophys Acta. 1971; 246:353–357. [PubMed: 5132910]

51. ter Schegget J, Flavell RA, Borst P. DNA synthesis by isolated mitochondria. 3. Characterization of D-loop DNA, a novel intermediate in mtDNA synthesis. Biochim Biophys Acta. 1971; 254:1–14. [PubMed: 4943979]
52. Robberson DL, Clayton DA. Replication of mitochondrial DNA in mouse L cells and their thymidine kinase - derivatives: displacement replication on a covalently-closed circular template. Proc Natl Acad Sci U S A. 1972; 69:3810–3814. [PubMed: 4509344]
53. Robberson DL, Kasamatsu H, Vinograd J. Replication of mitochondrial DNA. Circular replicative intermediates in mouse L cells. Proc Natl Acad Sci U S A. 1972; 69:737–741. [PubMed: 4501588]
54. Clayton DA. Replication of animal mitochondrial DNA. Cell. 1982; 28:693–705. [PubMed: 6178513]
55. Brown TA, Cecconi C, Tkachuk AN, Bustamante C, Clayton DA. Replication of mitochondrial DNA occurs by strand displacement with alternative light-strand origins, not via a strand-coupled mechanism. Genes Dev. 2005; 19:2466–2476. [PubMed: 16230534]
56. Yang C, Curth U, Urbanke C, Kang C. Crystal structure of human mitochondrial single-stranded DNA binding protein at 2.4 A resolution. Nat Struct Biol. 1997; 4:153–157. [PubMed: 9033597]
57. Wanrooij S, Falkenberg M. The human mitochondrial replication fork in health and disease. Biochim Biophys Acta. 2010; 1797:1378–1388. [PubMed: 20417176]
58. Delaney JC, Smeester L, Wong C, Frick LE, Taghizadeh K, Wishnok JS, Drennan CL, Samson LD, Essigmann JM. AlkB reverses etheno DNA lesions caused by lipid oxidation in vitro and in vivo. Nat Struct Mol Biol. 2005; 12:855–860. [PubMed: 16200073]
59. van Loon B, Hubscher U. An 8-oxo-guanine repair pathway coordinated by MUTYH glycosylase and DNA polymerase lambda. Proc Natl Acad Sci U S A. 2009; 106:18201–18206. [PubMed: 19820168]
60. Graham JM. Isolation of mitochondria from tissues and cells by differential centrifugation. Curr Protoc Cell Biol. 2001; Chapter 3 Unit 3 3.
61. O'Brien PJ, Ellenberger T. Human alkyladenine DNA glycosylase uses acid-base catalysis for selective excision of damaged purines. Biochemistry. 2003; 42:12418–12429. [PubMed: 14567703]
62. Longley MJ, Smith LA, Copeland WC. Preparation of human mitochondrial single-stranded DNA-binding protein. Methods Mol Biol. 2009; 554:73–85. [PubMed: 19513668]
63. Schurtenberger P, Egelhaaf SU, Hindges R, Maga G, Jonsson ZO, May RP, Glatter O, Hubscher U. The solution structure of functionally active human proliferating cell nuclear antigen determined by small-angle neutron scattering. J Mol Biol. 1998; 275:123–132. [PubMed: 9451444]
64. Henneke G, Koundrioukoff S, Hubscher U. Phosphorylation of human Fen1 by cyclin-dependent kinase modulates its role in replication fork regulation. Oncogene. 2003; 22:4301–4313. [PubMed: 12853968]
65. Fu D, Brophy JA, Chan CT, Atmore KA, Begley U, Paules RS, Dedon PC, Begley TJ, Samson LD. Human AlkB homolog ABH8 Is a tRNA methyltransferase required for wobble uridine modification and DNA damage survival. Mol Cell Biol. 2010; 30:2449–2459. [PubMed: 20308323]
66. Keller A, Nesvizhskii AI, Kolker E, Aebersold R. Empirical statistical model to estimate the accuracy of peptide identifications made by MS/MS and database search. Anal Chem. 2002; 74:5383–5392. [PubMed: 12403597]
67. MacCoss MJ, Wu CC, Yates JR 3rd. Probability-based validation of protein identifications using a modified SEQUEST algorithm. Anal Chem. 2002; 74:5593–5599. [PubMed: 12433093]
68. Wu Y, Li Q, Chen XZ. Detecting protein-protein interactions by Far western blotting. Nat Protoc. 2007; 2:3278–3284. [PubMed: 18079728]
69. Claros MG, Vincens P. Computational method to predict mitochondrially imported proteins and their targeting sequences. Eur J Biochem. 1996; 241:779–786. [PubMed: 8944766]
70. Nakai K, Horton P. PSORT: a program for detecting sorting signals in proteins and predicting their subcellular localization. Trends Biochem Sci. 1999; 24:34–36. [PubMed: 10087920]
71. Bannai H, Tamada Y, Maruyama O, Nakai K, Miyano S. Extensive feature detection of N-terminal protein sorting signals. Bioinformatics. 2002; 18:298–305. [PubMed: 11847077]

72. Xia L, Zheng L, Lee HW, Bates SE, Federico L, Shen B, O'Connor TR. Human 3-methyladenine-DNA glycosylase: effect of sequence context on excision, association with PCNA, and stimulation by AP endonuclease. J Mol Biol. 2005; 346:1259–1274. [PubMed: 15713479]

73. Radulovic M, Crane E, Crawford M, Godovac-Zimmermann J, Yu VP. CKS proteins protect mitochondrial genome integrity by interacting with mitochondrial single-stranded DNA-binding protein. Mol Cell Proteomics. 2010; 9:145–152. [PubMed: 19786724]

74. Curth U, Urbanke C, Greipel J, Gerberding H, Tiranti V, Zeviani M. Single-stranded-DNA-binding proteins from human mitochondria and Escherichia coli have analogous physicochemical properties. Eur J Biochem. 1994; 221:435–443. [PubMed: 8168532]

75. Wong TS, Rajagopalan S, Townsley FM, Freund SM, Petrovich M, Loakes D, Fersht AR. Physical and functional interactions between human mitochondrial single-stranded DNA-binding protein and tumour suppressor p53. Nucleic Acids Res. 2009; 37:568–581. [PubMed: 19066201]

76. Faith JJ, Pollock DD. Likelihood analysis of asymmetrical mutation bias gradients in vertebrate mitochondrial genomes. Genetics. 2003; 165:735–745. [PubMed: 14573484]

77. Stevnsner T, Nyaga S, de Souza-Pinto NC, van der Horst GT, Gorgels TG, Hogue BA, Thorslund T, Bohr VA. Mitochondrial repair of 8-oxoguanine is deficient in Cockayne syndrome group B. Oncogene. 2002; 21:8675–8682. [PubMed: 12483520]

78. Thorslund T, Sunesen M, Bohr VA, Stevnsner T. Repair of 8-oxoG is slower in endogenous nuclear genes than in mitochondrial DNA and is without strand bias. DNA Repair (Amst). 2002; 1:261–273. [PubMed: 12509245]

79. Fishel ML, Seo YR, Smith ML, Kelley MR. Imbalancing the DNA base excision repair pathway in the mitochondria; targeting and overexpressing N-methylpurine DNA glycosylase in mitochondria leads to enhanced cell killing. Cancer Res. 2003; 63:608–615. [PubMed: 12566303]

Abreviations

mtDNA	mitochondrial DNA
AAG	alkyladenine DNA glycosylase
mtSSB	mitochondrial single-stranded binding protein
ROS	reactive oxygen species
!A	1,N^6-ethenoadenine
AP	abasic site
BER	base excision repair
pol	DNA polymerase
TFAM	mitochondrial transcription factor A
APE	1apurinic/apyrimidinic endonuclease 1
MMS	methyl methanesulfonate

Highlights

- Alkyladenine DNA glycosylase (AAG) localizes to the mitochondria.
- AAG directly interacts with mitochondrial single-stranded binding protein (mtSSB).
- MtSSB suppresses AAG explicitly in the context of ssDNA, but not dsDNA.
- Interaction between AAG and mtSSB ensures lesion processing within dsDNA.

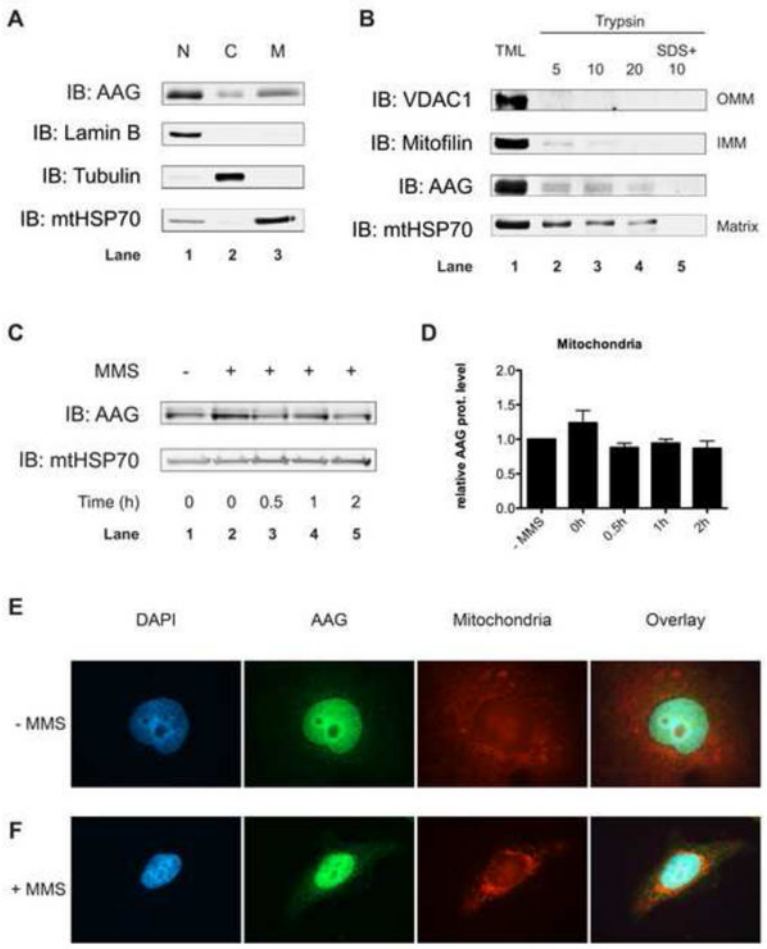

Figure 1. Human AAG localizes to the mitochondria, nucleus, and cytoplasm, and its cellular distribution is affected by MMS treatment

(**A**) Analysis of human AAG protein distribution in nuclear (N), cytoplasmic (C) and mitochondrial (M) fractions, prepared from HEK293T cells. Lamin B, Tubulin and mtHSP70 serve as loading control, as well as to ensure purity of the analyzed fractions. (**B**) Isolated mitochondria were treated for 1 h with the depicted amounts of trypsin (5, 10, or 20 μg/mL) and analyzed by immunoblot analysis. In lane 5. before trypsin treatment 0.1% SDS was added. In addition to AAG, we probed for: VDAC1 an outer mitochondrial membrane (OMM) marker, Mitofilin a marker of inner mitochondrial membrane (IMM) and mtHSP70, a mitochondrial matrix protein. TML represents total mitochondrial lysate obtained from purified mitochondrial fraction. (**C**) Immunoblot analysis of endogenous human AAG protein levels in mitochondrial fraction, obtained from mock or 2mM MMS treated HEK293T cells collected 0, 0.5, 1 or 2h after the treatment. (**D**) Quantification of AAG protein levels from three independently performed experiments like the one in (C). Relative AAG protein level is normalized to the level of mtHSP70. Error-bars represent SD values. (**E**) and (**F**) HeLa CCL2 cells synchronized in S-phase by double-thymidine block were pretreated with 100nM MitoTracker, followed by mock (E) or 2mM MMS (F) treatment. One hour after the treatment cells were stained with antibody against human AAG. The experiments were performed as described in *Experimental Procedures*.

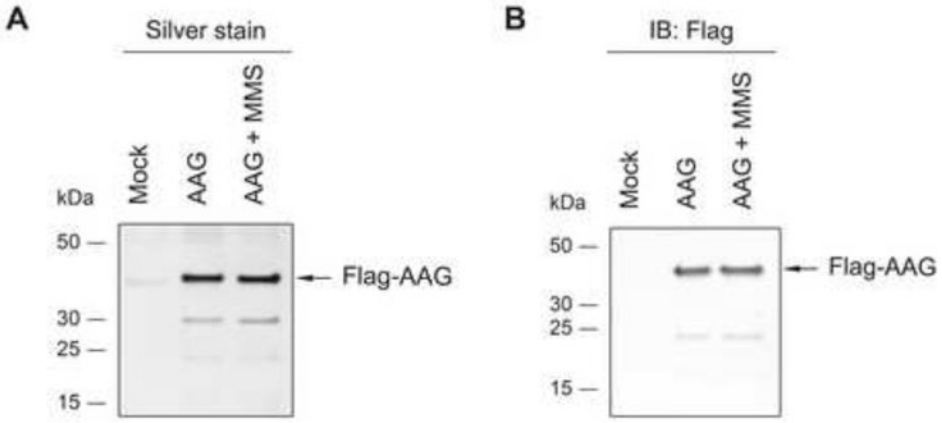

C

Protein	Accession	Purification			MW
		Mock	AAG	AAG + MMS	
		Unique number of peptides			
Alkyladenine DNA glycosylase	P29372	-	13	14	33
Proliferating cell nuclear antigen	P12004	-	5	6	29
Mitochondrial single-stranded DNA-binding protein	Q04837	-	-	3	17

Figure 2. MtSSB is detected in complex with human AAG

(**A**) Silver staining analysis of human AAG protein complexes purified from mock or 2mM MMS treated HEK293T cells. (**B**) Identification of Flag tagged AAG protein in purified fractions from (A) by immunoblot analysis. Arrows indicate the tagged AAG proteins. (**C**) LC-MS analysis of mitochondrial proteins that specifically co-purify with AAG. MtSSB is the only mitochondrial protein specifically identified in human AAG purifications. PCNA, a known-interacting partner of AAG is depicted as a positive control. The number of unique peptides indicates the number of unique spectra associated with a certain protein. The experiments were performed as described in *Experimental Procedures*.

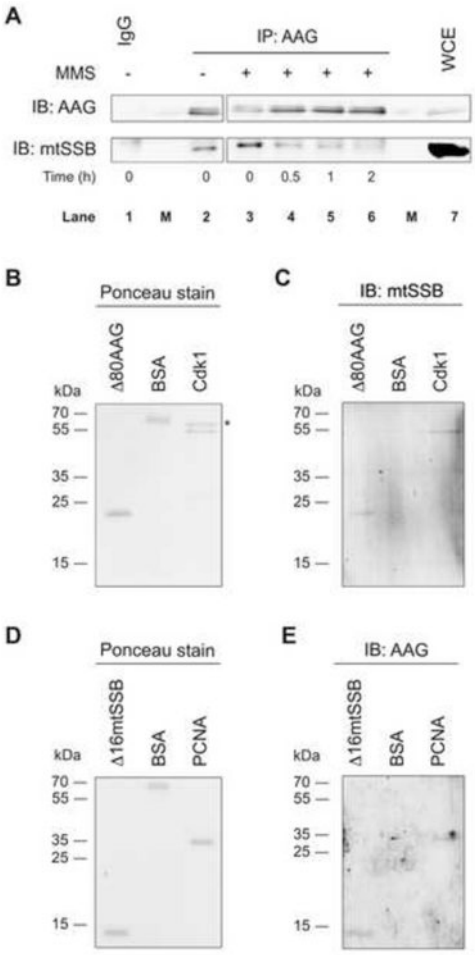

Figure 3. Human AAG and mtSSB proteins directly interact

(**A**) Immunoprecipitation of endogenous AAG and mtSSB proteins from extracts prepared from mock (lanes 1 and 2) or 2mM MMS treated (lanes 3-6) HEK293T cells, by using AAG antibody (lanes 2-6). "M" stands for protein markers. (**B**) Recombinant ! 80AAG, BSA and GST-Cdk1 proteins separated by SDS-PAGE, transferred to PVDF membrane and Ponceau stained. Star next to higher molecular band present in Cdk1 sample designates a contaminant protein co-purifying with Cdk1. (**C**) Interaction of ! 80AAG and His-!16mtSSB using far western blotting. Proteins on the PVDF membrane; ! 80AAG, BSA and GST-Cdk1 were denatured, renatured and then incubated with purified His-! 16mtSSB. After washing, bound protein was detected with mtSSB antibody. (**D**) Ponceau staining of recombinant His-!16mtSSB, BSA and His-PCNA proteins separated by SDS-PAGE and transferred to PVDF membrane. (**E**) Interaction between ! 80AAG and His-! 16mtSSB assessed by far western blotting. His-! 16mtSSB, BSA and His-PCNA proteins were denatured, renatured and then incubated with purified ! 80AAG. After washing, bound protein was detected with AAG antibody. The experiments were performed as described in *Experimental Procedures*.

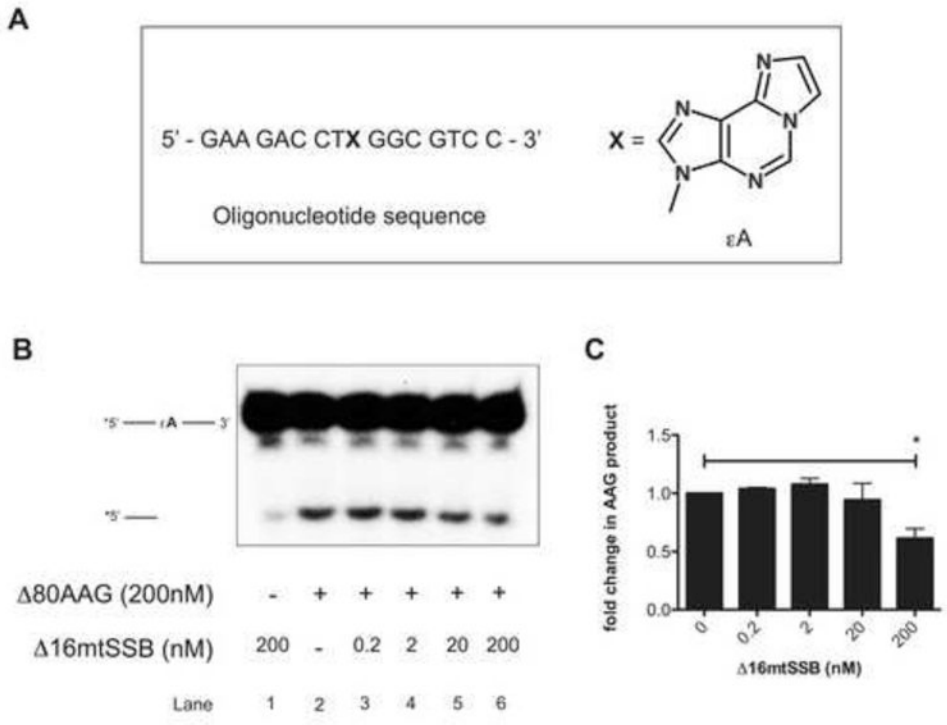

Figure 4. MtSSB inhibits AAG activity

(**A**) Schematic representation of 16-mer oligonucleotid used as a substrate in the DNA glycosylase and DNA binding assays. "X" designates 1,N^6-ethenoadenine (!A) lesion. To form dsDNA presented lesion-containing oligo nucleotide was annealed to the complementary undamaged DNA oligonucleotide. (**B**) Effect of ! 16mtSSB titration on the ! 80AAG glycosylase activity in the presence of 2nM !A ssDNA substrate. (**C**) Quantification of ! 16mtSSB effect on ! 80AAG glycosylase activity from three independently performed experiments like the one presented in (B) (error-bars represent SD values, *P<0.05). The experiments were performed as described in *Experimental Procedures*.

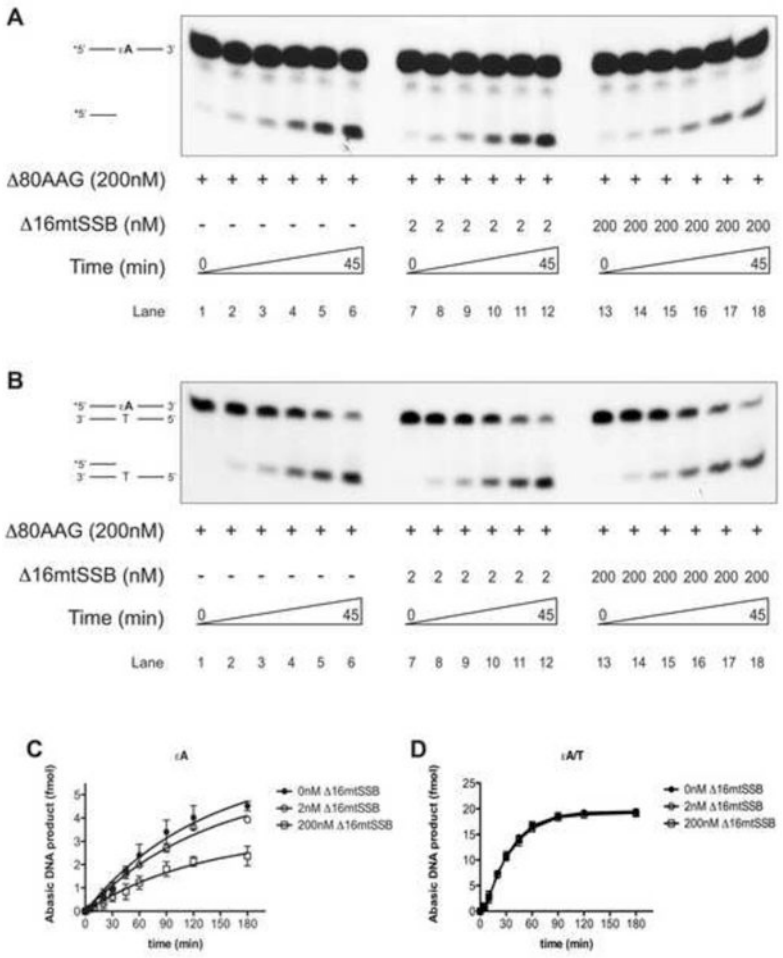

Figure 5. Inhibition of AAG activity by mtSSB is specific for single-stranded DNA

(**A**) and (**B**) Kinetic analysis of ! 80AAG glycosylase activity toward 2nM !A containing ssDNA (A) or dsDNA (B) substrate, in the absence or presence of ! 16mtSSB. (**C**) and (**D**) Quantification of AAG glycosylase activity in the presence of 0nM (!), 2nM (!) or 200nM (!) ! 16mtSSB, from three independently performed experiments, like the one presented in (A) and (B) respectively. The experiments were performed as described in *Experimental Procedures*.

Table 1
AAG isoforms A and B are potentially targeted to mitochondria

	Does isoform contain MTS*	Probability of import**	MTS**
AAG isoform A	YES	09764	MVTPALQMKKPKQFCRR
AAG Isoform B	YES	0.9804	MPARSGAQFCRR
AAG isoform C	NO	00919	-

Predication of AAG isoforms A, B and C targeting to mitochondria, as well as of their mitochondrial targeting sequences (MTS's); by iPSORT

*
and MitoProt II

**
software.

Table 2

Effect of ! 16mtSSB on kinetic constants of ! 80AAG mediated !A lesion excision from ssDNA and dsDNA

Δ16mtSSB	εA (ssDNA)		εA/T (dsDNA)	
	k_{obs} ± SD(min^{-1})[a]	initial excision rate (fmol/min)[b]	k_{obs} ± SD(min^{-1})[a]	initial excision rate (fmol/min)[b]
0nM	0.0076 ± 0.0011	0.048	0.0233 ± 0.0018	0.488
2nM	0.0074 ± 0.0008	0.041	0.0243 ± 0.0019	0.496
200nM	0.0076 ± 0.0016	0.025	0.0243 ± 0.0018	0.488

[a] Observed activity rate constants k_{obs} were determined from one-phase exponential association.

[b] The initial excision rate value is a result of the rate constant k_{obs} and the maximum saturation cleavage (maxiumum amount of AP product formed).